Synthesis and Characterization of Reactive Macroporous Poly(glycidyl methacrylate-triallyl isocyanurate-ethylene glycol dimethacrylate) Microspheres by Suspension Polymerization: Effect of Synthesis Variables on Surface Area and Porosity

Ata ur Rahman,[1] Mahmood Iqbal,[2] Faiz ur Rahman,[1] Dayan Fu,[1] Muhammad Yaseen,[1] Yongqin Lv,[1] Muhammad Omer,[3] Michael Garver,[4] Li Yang,[1] Tianwei Tan[1]

[1]*College of Life Science and Technology, Beijing University of Chemical Technology, Beisanhuan East Road No.15, Beijing 100029, People's Republic of China*
[2]*PCSIR, Karachi, Pakistan*
[3]*Department of Polymer Science & Engineering, Kyungpook National University, Daegu, South Korea*
[4]*State University of New York, College of Environmental Science and Forestry,1. Forestry Drive, Syracuse, New York 13210*

Received 19 December 2010; accepted 16 May 2011
DOI 10.1002/app.35026
Published online 11 October 2011 in Wiley Online Library (wileyonlinelibrary.com).

ABSTRACT: A novel macroporous poly(glycidyl methacrylate-triallyl isocyanurate-ethyleneglycol dimethacrylate) copolymer, hereinafter $P_{GMA\text{-}TAIC\text{-}EGDMA}$, of controlled bead size was prepared via free radical suspension copolymerization. The effects of varying the concentration of crosslinking agents and porogenic diluent on the average pore diameter, pore size distributions, specific surface area, and pore volume of the copolymer matrix were thoroughly investigated. The spherical beads were characterized by elemental analysis, Fourier transform infrared spectroscopy, and thermogravimetric analysis. The specific pore volume, average pore diameter, pore size distribution, and the specific surface area were measured by Mercury intrusion porosimetry and BET adsorption method, respectively. The porous properties of the polymer matrix are a direct consequence of the amount and quality of the porogenic solvent, the percentage of crosslinking monomers, and the ratio between the monomers and porogen phases. When the polymer was prepared at 30 and 40% crosslinking density, and 75 and 100% diluents, respectively, it showed a fine beads morphology, mechanical stability and pore size distributions. By comparing the copolymers $P_{GMA\text{-}TAIC\text{-}EGDMA}$ and $P_{GMA\text{-}EGDMA}$, it was found that the former is more stable both thermally and mechanically than its predecessor. The presence of epoxide functionalities of macroporous $P_{GMA\text{-}TAIC\text{-}EGDMA}$ beads makes it a versatile carrier. The resulting polymers have the potential for wide applications. © 2011 Wiley Periodicals, Inc. J Appl Polym Sci 124: 915–926, 2012

Key words: copolymerization; macroporous polymers; porous beads; resins; $P_{GMA\text{-}TAIC\text{-}EGDMA}$

INTRODUCTION

Macroporous polymers are characterized by their rigid porous matrix that perseveres in both the dry and swollen states. They are produced almost exclusively as spherical beads by conventional suspension copolymerization process. They have many applications in chromatography (gas chromatographs, high-performance liquid chromatography, gel permeation chromatography) and for the separation of biological compounds using modes such as reversed-phase, hydrophobic interaction, affinity, and ion-exchange chromatography, support for immobilization of enzymes in biosynthesis and carriers of classical catalysts. These polymers have also been used as adsorbents for the removal of metal ions (synthesis of selective complex-forming and chelating resins), solid-phase combinatorial and parallel synthesis, surface and groundwater purification, downstream treatment of organic chemical streams, and biochemical aqueous streams.[1–7] Various kinds of beaded homopolymers viz polymethacrylates, polystyrene, and heteropolymers or copolymers such as poly(styrene-divinylbenzene), poly(glycidyl methacrlate-divinlybenzene), poly(glycidyl methacrylate-ethylene glycol dimethacrylate), or $P_{GMA\text{-}EGDMA}$ and terpolymers like poly(GMA-HEMA-EGDMA) and poly (GMA-MMA-EGDMA) have been reported in the literature for this purpose.[1,2,8–17] Polymers having a functional group in its structural unit and capable of further transformations are termed as reactive polymers. The accessibility of this reactive group depends upon the type of compounds in which it is

Correspondence to: T. Tan (john.lotus@gmail.com).

present. In homogenously crosslinked polymers, the reactive groups are accessible for the agent only after sufficient swelling of the polymer matrix, that is, when polymer chains are sufficiently separated by action of osmotic forces. However, this presents a serious limitation to the selection of solvents applicable for the reactions. If the polymer matrix does not swell in a certain solvent, the reaction can occur only on the surface which contains only a slight amount of functional groups as compared with the whole polymer volume. A drawback of the homogeneously crosslinked polymers is also represented by slow diffusion of the reactant into the swollen polymer network and/or of reaction products from the polymer bulk.

The problems can be eliminated, to a remarkable extent, in heterogeneously crosslinked polymers which are characterized by a high porosity even in the dry state. Reactions of their functional groups occur on a large internal surface, usually independent of the thermodynamic quality of the solvent.[13,18] In some cases, the presence of reactive glycidyl methacrylate in these copolymers made them quite convenient for further changes. Glycidyl methacrylate (GMA) monomer has dual functionality, containing both methacrylic and epoxide groups. Both of these groups readily react with a wide range of monomers and functionalized molecules to provide the user with maximum freedom and flexibility in polymer design. The dual functionality of GMA also brings together the desirable properties of both methacrylics and epoxies.[19] However, their mechanical and thermal stability is not quite up to the mark.

This work was aimed to prepare a novel reactive macroporous poly(glycidylmethacrylate-triallylisocynurate-ethyleneglycoldimethacrylate) abbreviated as, $P_{GMA\text{-}TAIC\text{-}EGDMA,}$ copolymer matrix by suspension polymerization of reactive monomers to extend the range of applications and possibly to overcome drawbacks of existing materials. This kind of polymer matrix has not been reported in the literature so far. The new carrier is promising owing to the presence of trially isocyanurate as a crosslinker. Triallyl isocyanurate (TAIC) possesses some unique properties, it has a thermally stable triazine ring and allyl groups, providing a polymer with improved characteristics, including heat resistance, mechanical properties, and resistance to hydrolysis and weathering.[2] The TAIC and EGDMA were used as crosslinkers due their comparable reactivity and similarity with functional monomer GMA.

This article also investigates the influence of crosslinking density and porogen volume on the pore size, pore size distribution, specific pore volume, and surface area. Because, physicochemical parameters like, the level of crosslinker and the type and level of porogens, are very important in controlling the morphology and internal structure of the resulting copolymers.[20–22] These are the main variables which affect the porosity, specific pore volume, and surface area significantly.[23] In addition, the effect of stirrer speed on beads size distribution was also determined. The thermal and mechanical stabilities of $P_{GMA\text{-}EGDMA}$ and $P_{GMA\text{-}TAIC\text{-}EGDMA}$ were compared. The copolymers were extensively characterized by various techniques. The term "macroporous" in this article is used in the light of IUPAC rules versus the conventional sense. According to IUPAC definitions, the terms macropores, mesopores, and micropores are referred to pores having diameter >50 nm, 2–50 nm, and <2 nm, respectively.[24]

EXPERIMENTAL

Materials

The crosslinkers, EGDMA (98.0%) and TAIC (98.0%) were purchased from Acros Organics, New Jersey and were used without further purification. The functional monomer glycidyl methacrylate (GMA, 95.0%, stabilized with monomethyl ether hydroquinone (MEHQ)) was obtained from Tokyo Chemical Industry, Tokyo, Japan. The stabilizer PVA was purchased from Beijing Xudong Chemicals Factory; Beijing, China. The initiator 2, 2′-Azobisisobutyronitrile ($\geq$99%) was obtained from Sinopharm Chemical Reagent, Shanghai, China, and was purified by recrystallization from ethanol before use. All other reagents were of analytical grade from local suppliers and were used without further purification. Deionized water was used for making the aqueous phase.

Preparation of copolymer beads

The macroporous $P_{GMA\text{-}TAIC\text{-}EGDMA}$ copolymers were synthesized by suspension polymerization in a 500 mL trineck round bottom flask equipped with a mechanical stirrer and a reflux condenser under nitrogen atmosphere. The dispersed organic phase was comprised of 140 mmol ($\sim$ 22 mL), containing monomers mixture (GMA, TAIC, and EGDMA), azobisisobutyronitrile as an initiator (0.500 g) along with toluene and *n*-heptane as porogen (constant ratio of 9 : 1 vol % based on toluene for all series of copolymers). The above mixture was suspended in the aqueous continuous phase consisting of 250 mL of a 1% (w/v) aqueous solution of a suspension stabilizer PVA by agitation at 400 rpm optimized conditions under a nitrogen atmosphere at 45°C. The combined volume of the two liquid phases was chosen such that the height of the liquid was almost equivalent to the inner diameter of the reactor. The volumes of GMA and crosslinkers (TAIC and

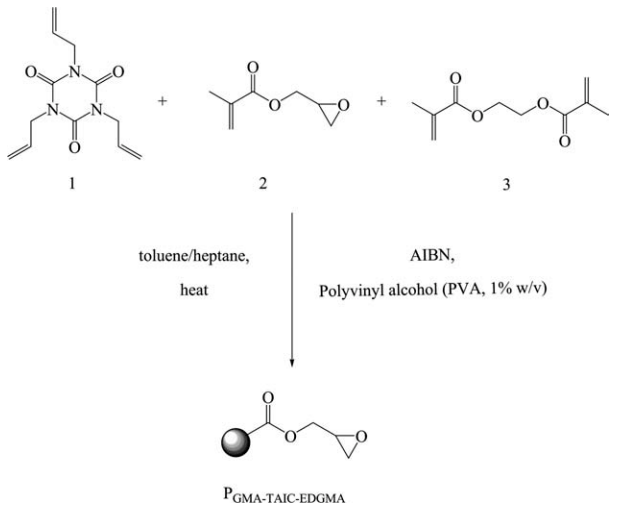

Scheme 1 Schematic representation of the copolymerization process.

EGDMA) were adjusted to a constant ratio for the monomer. The relative molar ratio between TAIC and EGDMA was always 1/1 (50/50%) and, this ratio was maintained constant in all the series of resins prepared. The size of the bead was controlled by adjusting the stirring speed after the required size of beads was attained. The contents of the reaction vessel were mixed using an anchor type stirrer powered by an IKA Eurostar Digital overhead stirrer (IKA-Werke GmbH and Co-KG, Staufen, Germany). The anchor type agitator was capable of radial mixing to prevent ingress and entrapment of air in the droplet, which could create artifacts due to uncontrolled additional voids/pores. The temperature of the suspension was then linearly raised from 45 to 65°C with a gradient of 0.33°C/min and was kept at 65°C for 1 h, then increased to 75°C in single step and maintained there for 2 h, and finally at 85°C for 2 h. The temperature regime was adjusted to make sure that the process did not occur too rapidly and to avoid formation of bubbles in the beads. Scheme 1 describes the copolymerization process. After completion of the reaction, the copolymer beads were filtered and washed thoroughly with hot water. Porogenic solvents in the beads were removed by ethanol in a Soxhlet extractor for 12 h. The copolymer beads were then dried *in vacuo* oven at 45°C for 24 h. Beads in the range of 106–250 μm were obtained for all series at 400 rpm, with exception of the effect of stirring speed on bead size, where the size of beads varies.

Several series of copolymers of differing crosslinking densities were synthesized at a constant volume of the inert diluent. Similarly, polymers of a specific composition i.e., crosslink density, were prepared with differing volumes of the porogen. Eight series of copolymers were synthesized at 10, 25, 50, 75, 100, 125, 150, and 200 vol % of porogen relative to the volume of the monomers, as presented in Tables I–VI. Here the mole percent of the crosslinking monomers relative to the moles of functional monomer or the mole ratio between the reactive monomer GMA and the crosslinkers (TAIC and EGDMA) is termed as crosslink density (CLD). The volume percent of the porogen in the organic phase is known as percent dilution. Since all the polymers were taken to the 100% conversion, the average CLD in all polymers is effectively the relative mole fraction of the crosslinking comonomer in the feed. Within each series, the crosslinking comonomers (TAIC and EGDMA) were varied at 10, 20, 30 40, 50, 75, and 100 mol % of (based on) glycidyl methacrylate. For the effect of stirring rate on bead size, the rpm was changed from 200 to 1000 for a specific copolymer having the same CLD and porogen volume as shown in Figure 1. To compare the composition, mechanical and thermal stabilities of $P_{GMA-TAIC-EGDMA}$ and $P_{GMA-EGDMA}$ copolymers, the latter was prepared by the same procedure as above with the concentration of diluent mixture and crosslinking density shown in Table V.

Physicochemical characterization

Fourier transform infrared spectroscopy

Infrared spectra from 4000 to 400 cm^{-1} were recorded on a Varian 3100 Fourier transform

TABLE I
Elemental Analysis Data of $P_{GMA-TAIC-EDGMA}$ Copolymer Matrix

	Elemental analysis[a]						Epoxy content		
	Theoretical value (calculated)			Actual value (experimental)			Functional monomer	Theoretical	Experimental
Polymer code	%C	%H	%N	%C	%H	%N	GMA (%)[b]	($mmolg^{-1}$)	($mmolg^{-1}$)
GTE-20/75	59.07	6.67	7.13	57.34	6.83	6.85	80	4.86	2.97
GTE-50/75	59.07	6.67	7.13	58.16	7.21	6.97	50	3.83	1.93
GTE-75/75	59.07	6.67	7.13	57.96	6.31	6.49	25	2.68	1.26

[a] Elemental analysis was calculated from multiple determinations within ±0.2% agreement.
[b] mol % of GMA in the feed.

TABLE II
Characteristics of Macroporous Copolymers Matrix Synthesized at 25% Porogen Volume (Series 1)

Serial No.	Polymer code	Crosslinking density (%)	Yield 106–250 μm (%)	Mean pore diameter[a] (D_p, nm)	Specific pore volume[b] (V_p, mL/g)	Specific surface area[c] (S_g, m^2/g)
1	GTE-25/10	10	80.7	123.6	0.53	10.2
2	GTE-25/20	20	82.2	105.4	0.55	13.2
3	GTE-25/30	30	85.6	97.3	0.56	16.4
4	GTE-25/40	40	87.3	91.7	0.59	18.6
5	GTE-25/50	50	83.6	85.4	0.62	22.3
6	GTE-25/75	75	81.4	78.2	0.69	25.2
7	GTE-25/100	100	78.1	71.6	0.73	29.1

[a] Mean pore diameter calculated from mercury porosimetry data.
[b] Pore volume determined by mercury intrusion porosimetry.
[c] Specific surface area calculated from the BET isotherm of nitrogen.

infrared Excalibur Series, spectrophotometer (Varian, Palo Alto, CA) and peaks are reported with resolution in reciprocal cm in the transmission mode. The polymer beads, 2 mg, was milled, mixed with potassium bromide (KBr), 100 mg, and pressed into a solid disk of 1.2 cm diameter prior to the infra-red measurement. A total of 40 scans were performed at a resolution of 1 cm^{-1} and the temperature of 21 ± 1°C.

Scanning electron microscopy

Surface morphology of the polymer matrix was observed using Hitachi *S*-4700, scanning electron microscope (Hitachi, Tokyo, Japan). Dried samples of $P_{GMA\text{-}TAIC\text{-}EGDMA}$ and $P_{GMA\text{-}EGDMA}$ copolymer beads were mounted on aluminum studs using adhesive graphite tape and sputter coated with approximately 10 nm of gold before analysis. For the inner structure of the matrix, beads were cut into pieces for inspection.

Mercury intrusion porosimetry

AutoPore IV 9500, mercury porosimeter from Micromeritics Instrument (Norcross, Georgia, USA) was used to determine the pore size distribution, mean pore diameter, and total pore volume of the copolymer beads. Samples were subjected to a pressure cycle starting at approximately 0.5 psia, increasing to 60,000 psia in predefined steps to give pore size/pore volume information.

N_2 Sorption porosimetry (BET)

N_2 sorption isotherms were generated using a ST-2000 surface area analyzer from Beijing Beifen Instrument Company, China. Samples were dried at 90°C for at least 6 h at high vacuum before sorption was started. The packaged software was used to compute copolymer specific surface areas using a BET model. The data obtained are summarized in Table I–VI.

Thermogravimetric analysis

Thermal stability and degradation of the polymers $P_{GMA\text{-}TAIC\text{-}EGDMA}$ and $P_{GMA\text{-}EGDMA}$ beads were determined by thermogravimetric analysis (TGA). TGA was carried out using TGA (Mettler-Toledo TGA/SDTA 851 e, Switzerland) with the Mettler STARe system. The measurement was typically carried out on 5.4 ± 0.4 mg size samples with a heat rate of 10°C/min from 30° to 800°C in a nitrogen atmosphere.

TABLE III
Characteristics of Macroporous Copolymers Matrix Synthesized at 50% Porogen Volume (Series 2)

Serial No.	Polymer code	Crosslinking density (%)	Yield 106–250 μm (%)	Mean pore diameter[a] (D_p, nm)	Specific pore volume[b] (V_p,mL/g)	Specific surface area[c] (S_g, m^2/g)
8	GTE-50/10	10	85.3	151.2	0.78	43.2
9	GTE-50/20	20	91.3	145.3	0.81	51.3
10	GTE-50/30	30	92.0	130.3	0.83	62.5
11	GTE-50/40	40	95.4	123.5	0.87	69.1
12	GTE-50/50	50	94.8	112.7	0.91	71.9
13	GTE-50/75	75	88.2	95.4	0.98	78.9
14	GTE-50/100	100	86.1	87.6	1.11	85.8

[a] Mean pore diameter calculated from mercury porosimetry data.
[b] Pore volume determined by mercury intrusion porosimetry.
[c] Specific surface area calculated from the BET isotherm of nitrogen.

TABLE IV
Characteristics of Macroporous Copolymers Matrix Synthesized at 75% Porogen Volume (Series 3)

Serial No.	Polymer code	Cross-linking density (%)	Yield 106–250 μm (%)	Mean pore diameter[a] (*Dp*, nm)	Specific pore volume[b] (*Vp*, mL/g)	Specific surface area[c] (*Sg*, m^2/g)
15	GTE-75/10	10	98.6	351.3	1.24	38.3
16	GTE-75/20	20	98.9	310.4	1.28	43.8
17	GTE-75/30	30	99.5	282.6	1.32	46.0
18	GTE-75/40	40	99.1	262.6	1.35	51.3
19	GTE-75/50	50	97.2	223.5	1.38	55.4
20	GTE-75/75	75	95.4	196.9	1.42	58.6
21	GTE-75/100	100	91.8	154.7	1.53	61.7

[a] Mean pore diameter calculated from mercury porosimetry data.
[b] Pore volume determined by mercury intrusion porosimetry.
[c] Specific surface area calculated from the BET isotherm of nitrogen.

Measurement of bead strength

The deformational characteristics of the individual beads in the dry state were measured at 20°C. An Instron Universal Testing Machine (Instron, Norwood, MA) was used to measure the mechanical properties of all samples in compression mode. A speed of 1 mm min^{-1} was used for all measurements. The planes compressing the bead were made of steel.[25–27] The force transducer had a maximal range of 10 kg, and the deformation indicator operated with the accuracy ± 0.0005 mm. Five samples of bead of approximately 200 μm in diameter were tested for each copolymer. The beads were loaded until a displacement of half the height of the examined bead was reached. The beads strength was expressed in MPa. The value of the compression stress and the Young's modulus were determined from an average of five samples.

Elemental analysis

The composition of the copolymers $P_{GMA\text{-}TAIC\text{-}EGDMA}$ and $P_{GMA\text{-}EGDMA}$ was analyzed using the PerkinElmer 2400 Series II CHNS/O Elemental Analyzer, in triplicate, after heating the samples at 100°C, under vacuum for 1 h. The theoretical and experimental percentage of carbon, hydrogen, and nitrogen is given in Table VII.

Determination of epoxy groups content. The content of epoxide groups was determined by volumetric titration as follows: the copolymer beads were dispersed in 0.1 mol/L tetraethyl ammonium bromide in acetic acid solution and titrated with a 0.1 mol/L perchloric acid solution in acetic acid until the crystal violet indicator changed to blue-green end point.[28]

RESULTS AND DISCUSSION

Synthesis of copolymer beads

Polymer particles were prepared by a standardized radical suspension copolymerization procedure. Once the polymerization conditions detailed in the Experimental Section were established, high-quality resin beads in the size range 106–250 μm were obtained consistently in high or very high yields. This confirms the effectiveness of polyvinyl alcohol as a robust stabilizer for the suspension copolymerization of these monomers. Series 7 and 8 being prepared at 10 and 200% volume of diluents, respectively, were not processed further due to poor beads quality and yield. Here, "% yield" can be defined as, the weight fraction of beads having diameter in the

TABLE V
Characteristics of Macroporous Copolymers Matrix Synthesized at 100% Porogen Volume (Series 4)

Serial No.	Polymer code	Crosslinking density (%)	Yield 106–250 μm (%)	Mean pore diameter[a] (D_p, nm)	Specific pore volume[b] (V_p, mL/g)	Specific surface area[c] (S_g, m^2/g)
22	GTE-100/10	10	97.8	534.7	1.52	34.2
23	GTE-100/20	20	98.6	513.7	1.58	38.4
24	GTE-100/30	30	99.6	503.8	1.63	39.6
25	GTE-100/40	40	99.4	486.8	1.68	42.7
26	GTE-100/50	50	97.4	460.1	1.73	45.8
27	GTE-100/75	75	94.1	443.9	1.81	49.6
28	GTE-100/100	100	91.5	421.9	1.88	52.9

[a] Mean pore diameter calculated from mercury porosimetry data.
[b] Pore volume determined by mercury intrusion porosimetry.
[c] Specific surface area calculated from the BET isotherm of nitrogen.

TABLE VI
Characteristics of Macroporous Copolymers Matrix Synthesized at 125% Porogen Volume (Series 5)

Serial No.	Polymer code	Crosslinking density (%)	Yield 106–250 μm (%)	Mean pore diameter[a] (D_p, nm)	Specific pore volume[b] (V_p, mL/g)	Specific surface area[c] (S_g, m^2/g)
29	GTE-125/10	10	75.9	2035	2.13	19.7
30	GTE-125/20	20	78.6	1198	2.21	23.5
31	GTE-125/30	30	83.5	1097	2.29	25.9
32	GTE-125/40	40	89.3	1016	2.32	27.4
33	GTE-125/50	50	91.8	981.9	2.39	30.6
34	GTE-125/75	75	93.1	851.7	2.46	34.9
35	GTE-125/100	100	94.2	757.7	2.52	38.4

[a] Mean pore diameter calculated from mercury porosimetry data.
[b] Pore volume determined by mercury intrusion porosimetry.
[c] Specific surface area calculated from the BET isotherm of nitrogen.

range of 106–250 μm. Physicochemical parameters such as the concentration of the crosslinking agent and type, composition, and concentration of the inert diluents mixture in the organic phase i.e., the ratio of monomers to porogens, can affect this yield. The data for the Series 1 to 6 of copolymer beads are documented in Tables I–VI. It can be observed that the yield of copolymer beads in Tables I–IV decreases beyond 40% CLD, this is probably associated with the increasing copolymerization rate owing to the increases in the molar concentrations of double bonds, thus resulting in beads with relatively large diameter and rough surfaces, similar results have been reported elsewhere.[29]

Effect of stirring rate on bead size distribution

Stirring speed plays a key role in particle size regulation. The higher the stirring speed, the smaller the beads size. Figure 1 shows the effect of stirring speed on the mean bead size for the copolymer GTE.75–40. It is obvious that particle size reduces significantly with an increase in agitation rate. The average particle size is 560, 200, and 80 μm at 200, 400, and 1000 rpm, respectively. Higher stirring intensity leads to particle disintegration at higher rpm because the probability of interactions between the beads is higher at increased stirring rates. The portion of smaller particles increases with increasing stirrer intensity. Smaller beads can find analytical use. Beads of sizes higher than 100 μm are suitable for preparative and industrial scale applications e.g., Amberlite, Dowex, etc. Beads of very large diameter are not suitable for use because of high diffusional constraints; it can hinder the transportation of reactants and products in the bulk of copolymer beads.

Characteristics of the copolymer beads

Fourier transform infrared spectroscopy spectroscopy. The composition of copolymer matrix was analyzed by Fourier transform infrared spectroscopy (FT-IR) spectroscopy and elemental analysis (EA). The FT-IR spectrum of a typical $P_{GMA\text{-}TAIC\text{-}EGDMA}$ (a) and $P_{GMA\text{-}EGDMA}$ (b) beads are presented in Figure 2 which ensured the presence of oxirane functionality and triazine ring of TAIC. The IR spectrum gave a prominent band at 1260 cm^{-1} due to the symmetrical stretching of the oxiranoyl ring.[8,30] Another band at 908 cm^{-1} due to epoxy ring out of plane vibration further confirmed the presence of epoxy group and hence GMA.[31] The distinguishing absorption band at 763 cm^{-1} is attributed to isotriazine ring of TAIC, in contrast no such band appeared in $P_{GMA\text{-}EGDMA}$, cf. (a) and (b) Figure 2.[32] Among the characteristic vibrations of both GMA and EGDMA is the methylene vibration at $\sim$ 2988 cm^{-1}. A doublet band at 1730 and 1698 cm^{-1} represents the ester configuration of both EGDMA and GMA, and TAIC, respectively. On the other hand, several bands appear in

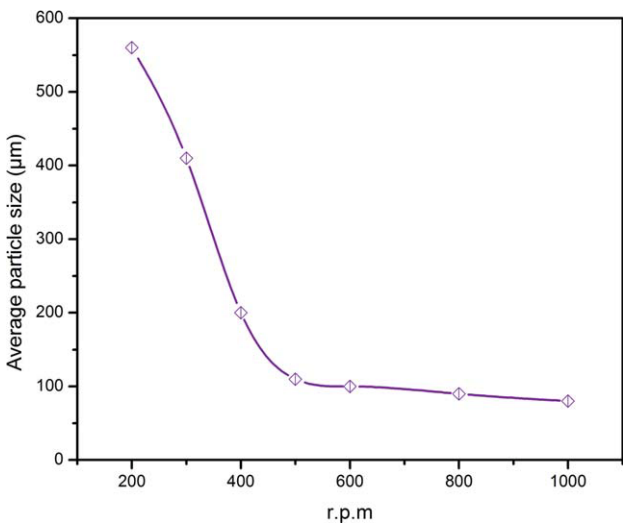

Figure 1 Effect of stirring rate on the mean particle size of the copolymer matrix. Crosslinking density 30%, porogen volume 100%. [Color figure can be viewed in the online issue, which is available at wileyonlinelibrary.com.]

TABLE VII
Characteristics of Macroporous Copolymers Matrix Synthesized at 150% Porogen Volume (Series 6)

Serial No.	Polymer code	Crosslinking density (%)	Yield 106–250 μm (%)	Mean pore diameter[a] (D_p, nm)	Specific pore volume[b] (V_p, mL/g)	Specific surface area[c] (S_g, m^2/g)
36	GTE-150/10	10	68.6	3118	2.65	3.7
37	GTE-150/20	20	72.4	3103	2.66	4.6
38	GTE-150/30	30	76.3	2956	2.71	6.4
39	GTE-150/40	40	78.0	2895	2.73	7.3
40	GTE-150/50	50	79.8	2794	2.79	7.1
41	GTE-150/75	70	81.6	2743	2.82	8.3
42	GTE-150/100	100	83.4	2643	3.01	9.6

[a] Mean pore diameter calculated from mercury porosimetry data.
[b] Pore volume determined by mercury intrusion porosimetry.
[c] Specific surface area calculated from the BET isotherm of nitrogen.

the finger print region for the samples between 1600 and 1200 cm^{-1}. These prominent absorption bands at 1150 and 1463 cm^{-1} are assigned to the —CH_2 scissoring and bending modes (δHCH) of both GMA and EGDMA, respectively. The broad absorption band at 3400–3600 cm^{-1} in both the spectra (a, b) can be attributed to the O—H stretching of hydrogen-bounded alcohol.[8,33]

Composition and oxirane content of $P_{GMA\text{-}Taic\text{-}Egdma}$ copolymer

The EA data for the $P_{GMA\text{-}TAIC\text{-}EGDMA}$ copolymer samples are presented in Table VII. The results show the presence of nitrogen in the copolymer matrix. The theoretical content of the elements in the synthesized $P_{GMA\text{-}TAIC\text{-}EGDMA}$, calculated on the basis of molecular formula of participating monomers is given for comparison. The EA data are in good agreement with these theoretical values. The difference is within the error limits of suspension polymerization. From the viewpoint of employing this reactive polymer to further conversions, it is important to know the actual content of accessible oxirane groups in the matrix. Epoxy content of the copolymer matrix which corresponds to mole % of GMA is also given in Table VII. The concentration of admissible epoxy groups not only depends on the GMA content in the feed or crosslinking density, and on the internal surface area, but also to a remarkable extent on the inert phase composition.[21] The epoxy groups content for the samples; GTE-20/75, GTE-50/75 and GTE-75/75 are 3.27, 2.93 and 1.86 mmol/g, respectively. The values drop with a reduction of GMA content in the feed.

Surface morphology and internal structure

The scanning electron micrographs of typical sample GTE-30/100 beads are depicted in Figure 3. The image shown in Figure 3(a) documents the shape, size, and surface morphology of the polymeric beads. It can be seen that the shape of bead is symmetric and strictly spherical with a narrow size distribution, and that the morphology of the surface is porous. The scanning electron microscopy (SEM) micrograph of a cross section of the bead depicts the internal structure of the bead [Fig. 3(b)] at a higher magnification. It clearly demonstrates the highly reticular, three dimensional porous matrix of the bead, which was formed by clusters of globules and numerous interconnected channels and pores. The globules in the bead are formed by the agglomerations of microspheres and microspheres are made by the coagulations of nuclei.[34] The pores show a rather large size distribution and appear to be interconnected by numerous channels in the pores walls, and pore diameter reaches up to 4 μm, moreover, globules having diameter in the range 100 to 300 nm can also be observed.

Effect of diluent concentration on beads porosity and surface area

A number of studies have been performed concerning the effects of variations in the concentration and

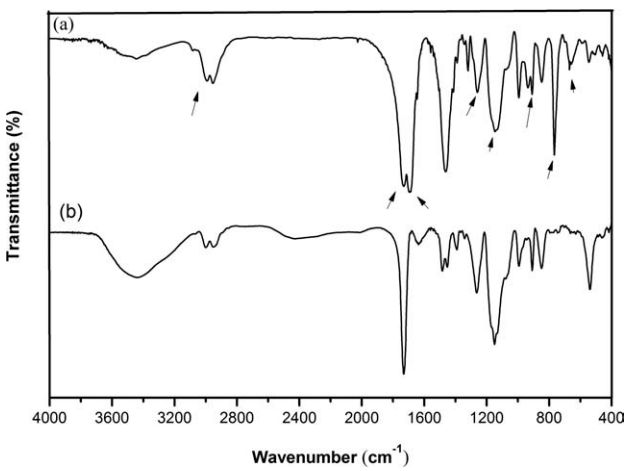

Figure 2 Comparison of the FT-IR spectra of the copolymer: (a) $P_{GMA\text{-}TAIC\text{-}EGDMA}$ and, (b) $P_{GMA\text{-}EGDMA}$.

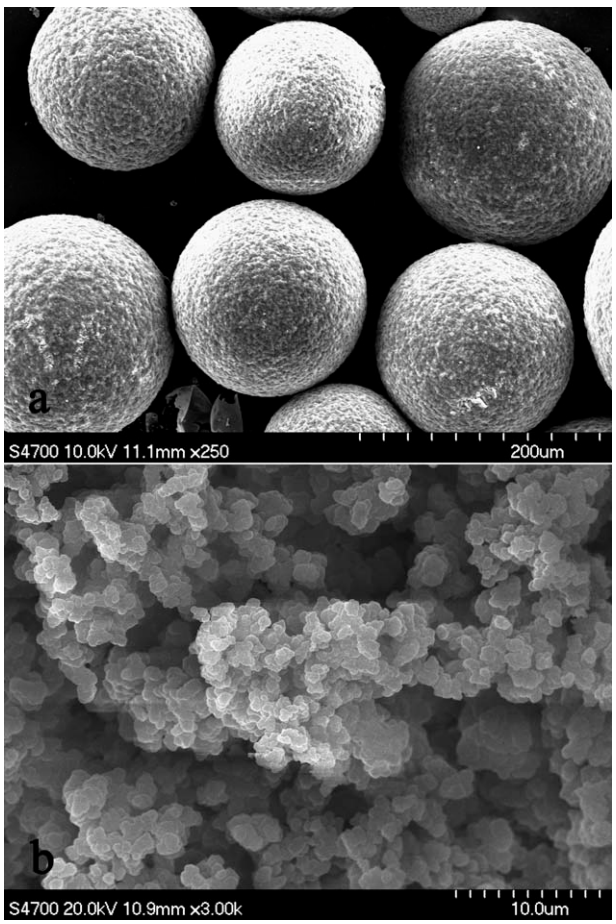

Figure 3 Scanning electron micrograph of the macroporous $P_{GMA\text{-}TAIC\text{-}EGDMA}$ Beads, Sample : GTE-30/100. (a) Morphology of microspheres at ×250, (b) cross section of a bead observed at a magnification of 3000.

type of diluent used.[1,34–37] For oil in water systems, the porogenic diluents are generally saturated hydrocarbons, aliphatic alcohols, and carboxylic acids. The pore size obtained will depend on the mutual solubility of the monomer mixture and the diluents, and the concentration, structure and polarity of the diluent. A porogen must be soluble in the organic phase, insoluble in the aqueous phase and perfectly chemically inert toward the various constituents of the mixture. Moreover, it must be easily extracted from the final copolymer. A mixture of toluene and heptane was chosen as the porogenic diluents; because of their good miscibility with the monomer mixture, for the synthesis of $P_{GMA\text{-}TAIC\text{-}EGDMA}$ copolymer. Toluene is a thermodynamically good solvent for the resulting polymer matrix and hence creates small pores. In contrast, use of a thermodynamically poor diluent such as heptane is known to yield polymer with modest surface area having macropores and a broad pore size distribution.[38] It was observed earlier that the addition of heptane to toluene used as porogenic solvent results in the formation of larger pores in poly(glycidylmethacrylate-triallylisocyanurate-ethylene dimethacrylate) beads.[32] This is also confirmed in this study. The details of composition and concentration of porogenic solvent and monomers used is described in the Experimental Section. Tables I–VI summarizes the results of BET nitrogen adsorption measurements and mercury intrusion porosimetry (MIP) for all copolymer matrices prepared.

Figure 4 depicts the effect of diluent concentration on the resulting surface area of the copolymer beads. If the concentration of the inert mixture in the dispersed phase is lower than 10 vol %, the matrices formed are nonporous spherical particles with an immeasurable specific surface area. This is because at low dilution of porogen a large number of nuclei are formed which tend to grow through each other and eventually result in low internal surface area.[39–41] There is a remarkable increase in surface area with increase in quantity of porogen from 10 to 50 vol %. This dramatic increase in surface area is due to porosity increase with diluents quantity. At the course of polymerization, monomers are transformed into a copolymer, while the inert solvents mixture fills up the pore space of the particles formed. The more inert components there are in the solvents mixture, the higher the porosity. After passing through a maximum, the curve moves downward. This trend can be explained on the basis of average pore diameter of the given polymers with constant crosslinking density, which is presented in Tables I–VI. It can be seen that diameter of the average pore increases monotonically with porogen concentration. The decrease in surface area beyond 50 vol % is due to this fact. Particles formed at 25% are quite strong due to low porosity. Beads formed

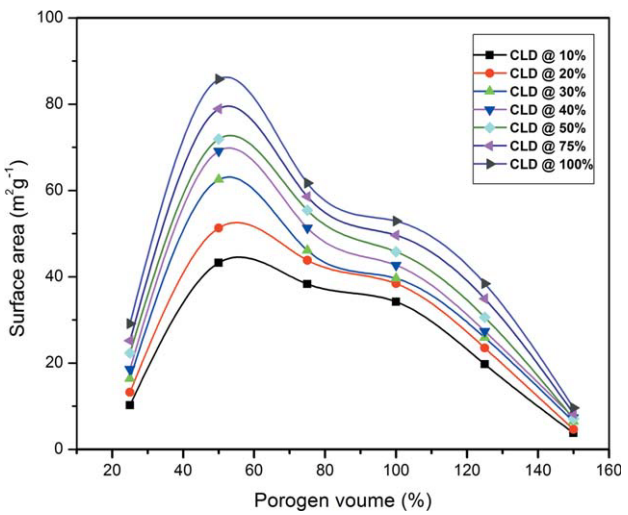

Figure 4 Effect of porogenic solvent concentration on the specific surface area of the resultant copolymer beads. CLD in legend shows the crosslinking density of different series. [Color figure can be viewed in the online issue, which is available at wileyonlinelibrary.com.]

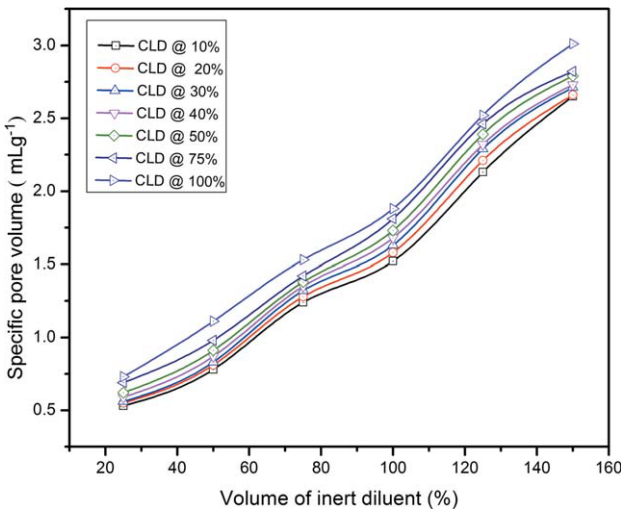

Figure 5 Effect of the concentration of porogenic solvent on the specific pore volume of copolymers prepared at different crosslinking densities. [Color figure can be viewed in the online issue, which is available at wiley onlinelibrary.com.]

below 100 vol % are much stronger mechanically than the beads formed at even higher concentration. Beads synthesized at 150 and 200 vol % are soft and easily collapsible due to large voids inside the beads structure. Figure 5 demonstrates the effect of diluents concentration on the specific pore volume. It can be observed that pore volume increases monotonically with increase in concentration of porogen. Similar results have been reported for other copolymer systems in the literature.[1,36] Log differential pore size distribution dv/day(logD) curves of the $P_{GMA\text{-}TAIC\text{-}EGDMA}$ beads as measured by MIP, for the samples being prepared at 30% crosslinking density and is shown in Figure 6. It is obvious that the lognormal pore size distributions shift toward larger pore diameter with an increase in the concentration of diluent.

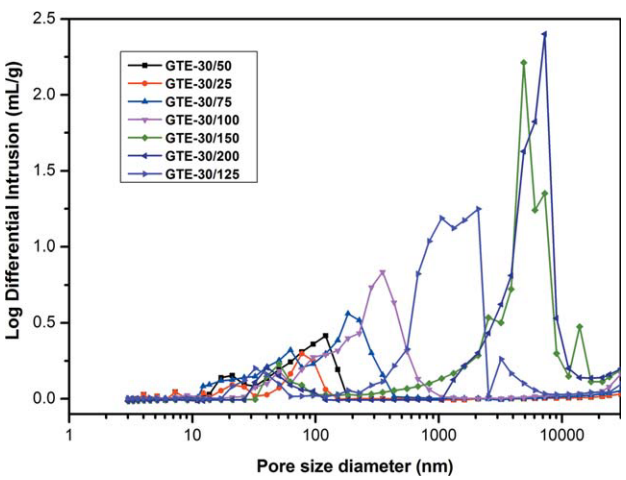

Figure 6 Log differential pore size distribution [dv/day ($LogD_p$)] curves of the $P_{GMA\text{-}TAIC\text{-}EGDMA}$ beads as measured by MIP. Legends show the copolymer samples. Crosslinking density, 30%. Volume of porogen, 25 to 200 vol % based on monomers. [Color figure can be viewed in the online issue, which is available at wiley onlinelibrary.com.]

Effect of crosslinking density on beads porosity and surface area

Crosslinking density plays an important role because it not only affects the chemical properties but also the physical characteristics of the final copolymer matrix. Varying the concentration of crosslinker leads to a polymer with different chemical composition and hence different characteristics. For instance, increasing the percentage of crosslinker results in lower concentration of functional monomer GMA and indirectly to epoxide groups' content. The data of surface area, average pore diameter and specific pore volume obtained from the nitrogen sorption isotherm and mercury porosimetry for the copolymers synthesized at 25, 50, 75, 100, 125,150, vol % of diluents are given in Tables I–VI (Series 1-6). The first series GTE-20/10 to GTE-25/100 employed 10, 20, 30, 40, 50, 75, and 100 mol % of crosslinker and 25 vol % of porogen. Surface area is observed to increase with crosslinking density at constant diluent concentration as shown in Figure 7. The same phenomena are noted for all series but in different magnitude because each series is being synthesized at different amount of porogen. The increase in surface area with crosslinker concentration is due to a decrease in the size of the microspheres which itself are formed by the agglomerations of nuclei inside a bead.[36,39–42] The portion of the defective particles

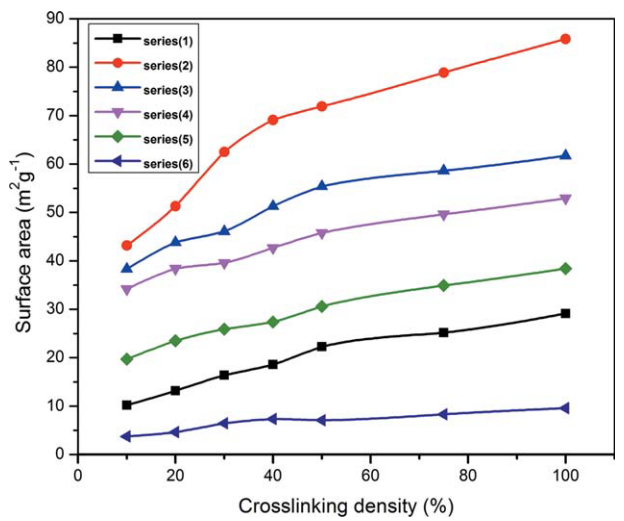

Figure 7 Effect of crosslinker concentration on the specific surface area of copolymers at different percent dilutions. [Color figure can be viewed in the online issue, which is available at wileyonlinelibrary.com.]

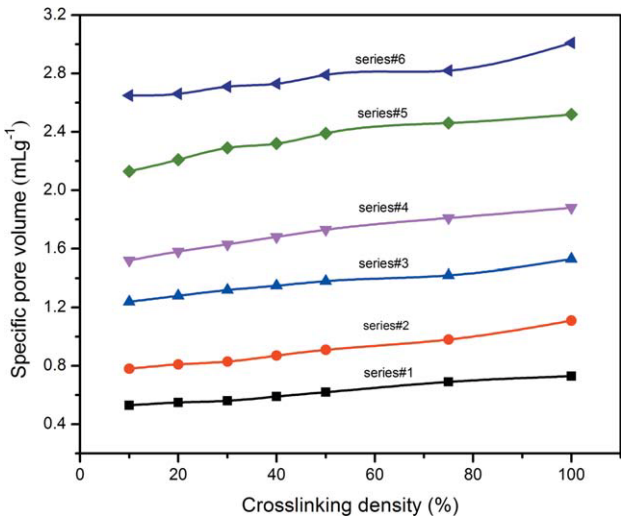

Figure 8 Effect of the mole fraction of crosslinking agent on the specific pore volume as determined by MIP. [Color figure can be viewed in the online issue, which is available at wileyonlinelibrary.com.]

increased with the content of the crosslinking agent in the feed. This is probably associated with the increasing polymerization rate owing to the increases in molar concentrations of double bonds. Moreover, for every series the specific pore volume increases with an increase in crosslinking density. This trend is summarized in Figure 8, a plot of pore volume against crosslinking density. Each curve is representative of pore volume relative to crosslinking density for a particular volume of porogen. It can be observed from Figure 8 that the effect of polymer composition is not as significant as that of diluents concentration on the pore volume of the copolymers.

In a nutshell, a polymer prepared at 30–40 mol % crosslinking density and 70–100 vol % porogen provide the best chemical and physical characteristics like, surface area, specific pore volume, pore size distribution, content of epoxy groups, and mechanical stability. Mole fractions of crosslinker higher than 50% leads to poor bead morphology and compromised epoxide content, on the contrary, lower mole fractions of crosslinker (<20%) causes weaker beads with respect to mechanical and thermal stability (discussed in Section 3.8). Beads prepared at porogen concentrations higher than 100 vol %, resulted in soft and easily collapsible beads structure, while copolymers synthesized at lower diluent concentrations do not provide the desired essential parameters, like specific pore volume, pore size distribution, and surface area for the final polymer matrix.

Comparison of the mechanical and thermal stability of the beads

A comparison of the mechanical stabilities of $P_{GMA\text{-}EGDMA}$ and $P_{GMA\text{-}TAIC\text{-}EGDMA}$ copolymers are shown in Table VIII. The comparing pairs of the copolymers have the same concentration of crosslinker and inert porogenic solvent. It can be observed that the penetration modulus and stress at break of the copolymer beads increases with increasing in the concentration of the crosslinking agent (Table VIII, polymer 1-3). Increase in crosslinking density results in a finer globular structure of heterogeneous polymers and, hence mechanically strong and more rigid beads. For pairs of beads with the same crosslinking density and diluent concentration, the $P_{GMA\text{-}TAIC\text{-}EGDMA}$ beads are much stronger than the corresponding $P_{GMA\text{-}EGDMA}$ beads due to the presence of TAIC as a robust crosslinker in the former. The effect of porogen volume on the mechanical properties of the two copolymers is also presented in Table VIII. It is clear that at constant crosslinker concentration the mechanical stability of

TABLE VIII
Characteristics of the Copolymers: Comparison of Thermal and Mechanical Stability

			Mechanical stability						Thermal stability	
			$P_{GMA\text{-}EGDMA}$			$P_{GMA\text{-}TAIC\text{-}EGDMA}$			$P_{GMA\text{-}EGDMA}$	$P_{GMA\text{-}TAIC\text{-}EGDMA}$
Copolymer	Porogenvolume (Vol %)	Crosslinking density (mol %)	A^a (MPa)	$\sigma_b{}^b$ (MPa)	$\lambda_b{}^c$	A^a (MPa)	$\sigma_b{}^b$ (MPa)	$\lambda_b{}^c$	T_{onset} (°C)[d]	T_{onset} (°C)[d]
1	75	20	20.4	15.6	0.31	32.7	22.3	0.35	246	275
2	75	50	32.6	26.3	0.35	43.4	37.2	0.38	257	293
3	75	75	41.7	37.1	0.39	56.8	44.9	0.41	278	311
4	25	40	223	186	0.51	295	251	0.53	254	289
5	75	40	31.2	25.7	0.37	45.2	36.7	0.37	255	285
6	125	40	6.41	5.21	0.25	9.71	7.83	0.29	253	287

[a] Penetration modulus.
[b] Stress at break
[c] Relative compression at break.
[d] Temperature at the onset of decomposition.

the resultant beads decreases with increase in the concentration of diluents due to higher porosity. If the content of inert solvents and, consequently, the porosity is higher, the surface shell is less compact and the penetration modulus A and the stress at break $\sigma_{b,}$ are lower than those observed with less porous samples. The strain at break E_b does not depend on the content of the inert solvents to any considerable extent. Extreme values for modulus A and stress at break σ_b and an unusually compact submicroscopic structure can be observed in polymer 4. When prepared at low concentration of the inert mixture and high interfacial tension, the system is more rigid. Comparing the copolymers pairs at the same crosslinking density shows that, the polymer prepared with TAIC as a crosslinker provide more rigidity to the copolymer system in $P_{GMA\text{-}TAIC\text{-}EGDMA}$.

Table VIII provides an insight into the thermal stabilities of the two copolymers compared at various concentrations of diluents and crosslinker. For assessing relative thermal stability of polymers with different compositions, bead samples were characterized by determining the onset temperature of decomposition. TGA data shows that, the T_{onset} increases with increasing concentration of crosslinking agent (copolymer 1, 2, and 3). Pairs of the beads of the two copolymers having the same crosslinking density show that $P_{GMA\text{-}TAIC\text{-}EGDMA}$ is more stable thermally than $P_{GMA\text{-}EGDMA}$ due to the presence of trially isocyanurate as a crosslinker. This phenomenon cab be explained by the following mechanism; the inherent instability of all polyMETHacrylates arises from the low-ceiling temperature Tc of these monomers. The consequence of this is that if a terminal radical is formed on a polyMETHacrylate chain at modest temperatures above the Tc the polymer chain "unzips" to form monomer molecules. So serious is this that commercially produced polymethylMETHacrylate (PMMA, Perspex) has to be stabilized by including some methyl acrylate (or other acrylate) in the polymerization. The acrylate segments minimize any tendency to "unzip" because terminal free radicals are able to abstract the backbone H atom in the acrylate segments forming a relatively stabilized tertiary radical. PolyMETHacrylates therefore would be expected to have improved thermal stability in the presence of other groups capable of yielding an H atom to abstraction. One such group is the allyl group, of which there are three in TAIC. Allyl monomers polymerize only with difficulty because propagating radicals tends to abstract the allylic atoms forming stable allyl radicals in preference to adding to the allyl C=C bond. Polymers formed with TAIC contain some unreacted allyl groups and these would act as excellent free radical traps in the $P_{GMA\text{-}TAIC\text{-}EGDMA}$ terpolymer. Thus, the improved thermal stability of these polymers can be attributed to the above mechanism. Increasing the porogen concentration at constant crosslinking density does not affect the T_{onset} value for copolymers 5, 6, and 7, because all these samples have the same chemical composition.

CONCLUSIONS

In this study, a novel reactive macroporous $P_{GMA\text{-}TAIC\text{-}EGDMA}$ copolymer of controlled bead size was prepared via free radical suspension copolymerization. Toluene and *n*-heptane was used as porogen. The effect of the concentration of crosslinking agent and porogenic diluent on the average pore diameter, pore size distributions, specific surface area and pore volume of the copolymer matrix were thoroughly investigated. The EA and FT-IR spectroscopy confirmed that the copolymer is a matrix of GMA, TAIC, and EGDMA. The SEM data revealed the excellent morphology and highly reticular internal structure. The porous properties of the polymer matrix was a direct consequence of the amount and quality of the porogenic solvent, as well as the percentage of crosslinking monomers and the ratio between the monomers and porogen phases. Copolymers prepared at 30 and 40% crosslinking density, and 75 and 100% diluent, respectively, showed a fine bead morphology, mechanical stability and pore size distributions. Beads prepared at higher crosslinker concentrations were mechanically stable but their bead morphology was not satisfactory, similarly beads synthesized at 125 or higher vol % of diluent were not strong enough to withstand mechanical stresses due large pores in their structure. We also documented that the copolymer $P_{GMA\text{-}TAIC\text{-}EGDMA}$ was more stable both thermally and mechanically than its predecessor $P_{GMA\text{-}EGDMA}$. The copolymer can be customized further thanks to the presence of versatile epoxy groups. The resulting polymers can find many applications in chromatography, immobilization of biomolecules, solid phase organic synthesis, separation, etc.

The authors acknowledge the financial supports obtained from the National Natural Science Foundation of China (20636010, 50373003, and 20406002), 863 program (2006AA02Z245, 2007AA100404), 973 program (2007CB714305), Beijing Scientific and Technological Program (D0205004040211).

References

1. Ferreira, A.; Bigan, M.; Blondeau, D. React Funct Polym 2003, 56, 123–136.
2. Zhou, X.; Xue, B.; Sun, Y. Biotechnol Prog 2008, 17, 1093–1098.
3. Lei, Y.; Liu, Z.; Liu, Q.; Wu, X. React Funct Polym 2001, 48, 159–167.
4. Hrubý, M.; Hradil, J.; Benes, M. J. React Funct Polym 2004, 59, 105–118.

5. Onjia, A.; Milonjic, S. K.; Jovanovic, N. N.; Jovanovic, S. M. React Funct Polym 2000, 43, 269–277.
6. Maurya, M.; Sikarwar, S.; Joseph, T.; Manikandan P. Halligudi, S. React Funct Polym 2005, 63, 71–83.
7. Dofner, K.; de Gruyter, W. Ion Exchangers; Berlin, Germany, 1991.
8. Çaykara, T. J Appl Polym Sci 2007, 106, 2126–2131.
9. Lu, J.; Toy, P. H. Chem Rev 2009, 109, 815–838.
10. Hoaiand, N. T.; Kim, D. AIChE J 2009, 55, 3248–3254.
11. Atia, A. A.; Donia, A. M.; Elwakeel, K. Z. React Funct Polym 2005, 65, 267–275.
12. Arica, M. Y.; Bayramoglu, G.; Biçak, N. Proc Biochem 2004, 39 2007–2017.
13. Bayramoglu, G.; Kaya, B.; Arica, M. Y. Food Chem 2005, 92, 261–268.
14. Ahmed, M.; Malik, M. A.; Pervez, S.; Raffiq, M. Eur Polym J 2004, 40, 1609–1613.
15. Arrua, R. D.; Moya, C.; Bernardi, E.; Zarzur, J. Strumia, M.; Igarzabal, C. I. A. Eur Polym J 2010, 46, 663–672.
16. Horák, D.; Pollert, E.; Trchová, M.; Kovárová, J. Eur Polym J 2009, 45, 1009–1016.
17. Zhou, W.-Q.; Gu, T.-Y.; Su, Z.-G.; Ma, G.-H. Eur Polym J 2007, 43, 4493–4502.
18. Jovanović, S. M.; Nastasović, A.; Jovanović, N.; Jeremić, Z.; Savić, Z. Angewandte Makromolekulare Chemie 1994, 219, 161–168.
19. Horák, D.; Straka, J.; Stokr, J.; Schneider, B.; Tennikova, T. B.; Svec, F. Polymer 1991, 32, 1135–1139.
20. Dowding, P.; Vincent, B. Colloid Surface A 2000, 161, 259–269.
21. Okay, O. Prog Polym Sci 2000, 25, 711–779.
22. Kotha, A.; Raman, R. C.; Ponrathnam, S.; Shewale, J. G. React Funct Polym 1996, 28, 227–233.
23. Sherrington D. Chem Commun 1998, 2275, 1998.
24. Rouquerol, J.; Avnir, D.; Fairbridge, C. W.; Everett, D. H.; Haynes, J. M.; Pernicone, N.; Ramsay, J. D. F.; Sing, K. S. W.; Unger, K. K. Pure Appl Chem 1994, 66, 1739.
25. Peska, J.; Stamberg, J.; Hradil, J.; Ilavsk, M. J Chromatogr A 1976, 125, 455–469.
26. Couroyer, C.; Ning, Z.; Ghadiri, M.; Brunard, N.; Kolenda, F.; Bortzmeyer, D.; Laval, P. Powder Technol 1999, 105, 57–65.
27. Egholm, R.; Christensen, S.; Szabo, P. J Appl Polym Sci 2006, 102, 3037–3047.
28. Jay, R. Analytical Chem 1964, 36, 667–668.
29. Pulko, I.; Krajnc, P. Acta Chimica Slovenica 2005, 52, 215.
30. Field, J.; Cole, J.; Woodford, D. J Chem Phys 1950, 18, 1298.
31. Skaria, S.; Rajan C. Ponrathnam, S. Polymer 1997, 38, 1699–1704.
32. Yu, Y.; Sun, Y. J Chromatogr A 1999, 855, 129–136.
33. Bayramoglu, G.; ArIca, M. Y. J Mol Catal B Enzym 2008, 55, 76–83.
34. Jacobelli, H. Bartholin M.; Guyot, A. Die Angewandte Makromolekulare Chemie 1979, 80, 31–51.
35. Horák, D.; Lednick, F.; Bleha, M. Polymer 1996, 37, 4243–4249.
36. Kotha, A.; Raman, R.; Ponrathnam, S.; Shewale, J. React Funct Polym 1996, 28, 227–233.
37. Coutinho, F. M. B.; Torre, M. L. L.; Rabelo, D. Eur Polym J 1998, 34, 805–808.
38. Durie, S.; Jerabek, K.; Mason, C.; Sherrington, D. Macromolecules 2002, 35, 9665–9672.
39. Guyot, A. Syntheses and Separations Using Functional Polymers, Wiley, Chichester, 1988; pp 1–42.
40. Hall, P. J.; Machado, W. R.; Galan, D. G.; Barria, E. B.; Sherrington, D. C. J Chem Society 1996, 92, 2607–2610.
41. Hall, P. J.; Gascon Galan, D.; Ruiz Machado, W.; Mondragon, F.; Barrientos Barria, E.; Sherrington, D. C.; Calo, J. M. J Chem Society 1997, 93, 463–466.
42. Horák, D.; Šec, F.; Ilavský, M.; Bleha, M.; Baldrián, J.; Kálal, J. Die Angewandte Makromolekulare Chemie 1981, 95, 117–127.